AIP | Review of Scientific Instruments

Installation of soft X-ray array diagnostics and its application to tomography reconstruction using synthetic KSTAR X-ray imagesa)

Seung Hun Lee, Juhyeok Jang, Joohwan Hong, D. Pacella, A. Romano, L. Gabellieri, Siwon Jang, Junghee Kim , and Wonho Choe

Citation: Review of Scientific Instruments **85**, 11E827 (2014); doi: 10.1063/1.4896960
View online: http://dx.doi.org/10.1063/1.4896960
View Table of Contents: http://scitation.aip.org/content/aip/journal/rsi/85/11?ver=pdfcov
Published by the AIP Publishing

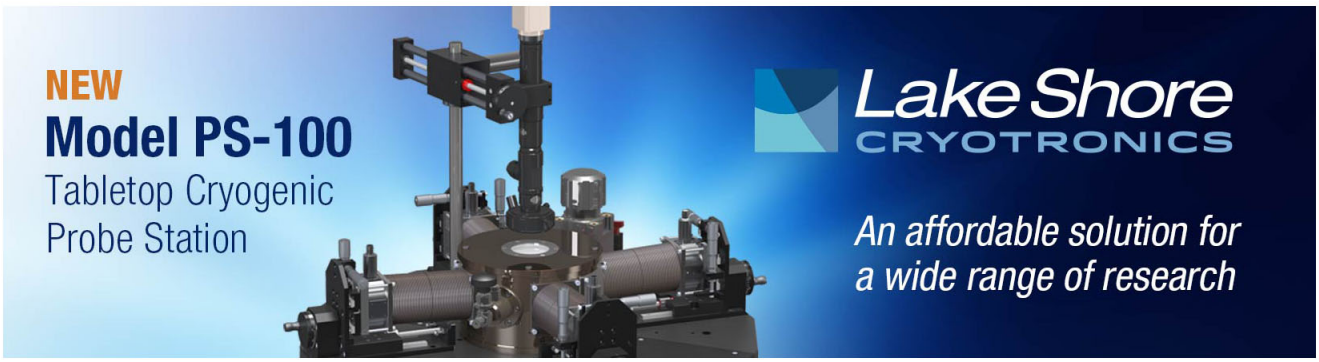

Installation of soft X-ray array diagnostics and its application to tomography reconstruction using synthetic KSTAR X-ray images[a)]

Seung Hun Lee,[1,2] Juhyeok Jang,[1,2] Joohwan Hong,[1,2] D. Pacella,[3] A. Romano,[3] L. Gabellieri,[3] Siwon Jang,[1,2,b)] Junghee Kim,[4,5] and Wonho Choe[1,2,c)]
[1]*Department of Physics, Korea Advanced Institute of Science and Technology, Daejeon 305-701, Republic of Korea*
[2]*Impurity and Edge Research Center, Daejeon 305-701, Republic of Korea*
[3]*Associazione Euratom-ENEA sulla Fusione, C.R. Frascati 00044, Italy*
[4]*National Fusion Research Institute, Daejeon 305-806, Republic of Korea*
[5]*Major of Nuclear Fusion and Plasma Science Department, Korea University of Science and Technology, Daejeon 305-350, Republic of Korea*

(Presented 5 June 2014; received 1 June 2014; accepted 18 September 2014; published online 16 October 2014)

Four-array system of soft X-ray diagnostics was installed on KSTAR tokamak. Each array has 32 viewing chords of two photo-diode array detectors with spatial resolution of 2 cm. To estimate signals from the soft X-ray radiation power, typical n_e, T_e, and argon impurity line radiation profiles in KSTAR are chosen. The photo-diodes were absolutely calibrated as a function of the incident photon energy in 2–40 keV range with a portable X-ray tube. Two-dimensional T_e image properties by multi-energy method were simulated and visualized with six combinations of beryllium filter sets within the dynamic range of signal ratio. © *2014 AIP Publishing LLC*. [http://dx.doi.org/10.1063/1.4896960]

I. INTRODUCTION

Various tomography reconstruction methods have been developed for KSTAR soft X-ray (SXR) array diagnostics.[1–3] It is discovered that at least four-array system is essential for elongated plasmas and six-array system is required to reconstruct hollow-shaped plasmas.[1] Since the two-array SXR diagnostic system could not satisfy magnetics-free reconstruction,[4] four-array SXR diagnostic system have been additionally developed, installed, and prepared for the 2014 KSTAR experimental data acquisition. There are two horizontal and two vertical arrays in *Z*-plane symmetry, and each array has 32 viewing chords of two photo-diode array detectors with spatial resolution of 2 cm. In a single chord, two different channels are designed to look at the same plasma volume penetrating beryllium (Be) filters of different thicknesses, in order to apply the multi-energy method.[5]

The photo-diode detector used in the four-array SXR diagnostic system in KSTAR is AXUV-16ELG, which is widely used for X-ray detection in other tokamak devices.[6,7] To measure the soft X-ray radiation power emitted from KSTAR plasmas, the responsivity of AXUV-16ELG is essential as a function of incident photon energy. The responsivity value is already demonstrated in Opto Diode Corp. website.[8] However, the calibration of each detector element should be confirmed since each feature of the detector could not be identical in active area and/or effective thickness. In this work, an X-ray tube with silver anode was used for the X-ray calibration, in order to simulate the plasma conditions as an X-ray source with abundant bremsstrahlung. The spectra of the X-ray tube were obtained by reconstruction of experimental data with a Si p-i-n spectroscopic detector. Total number of photons impinging on the AXUV detector can be easily calculated from the source spectrum and the detector responsivity. In order to find out the detector responsivity, the photo-current produced by an AXUV detector should be compared with total number of photons calculated by a certain detector responsivity. If the change of photo-current is measured with various spectra of the X-ray tube, the detector responsivity curve can be derived empirically. Additionally, the relative calibration factors among every 256 AXUV detectors are determined in a fixed condition of the X-ray tube.

The signal estimation of the four-array SXR diagnostic system is important to determine the current-to-voltage gain of the preamplifier for the photo-diodes. In this research, the typical electron density (n_e) and electron temperature (T_e) in KSTAR L-mode and H-mode cases were introduced to create synthetic continuum X-ray radiation models. Furthermore, the argon (Ar) impurity line radiation was considered under the condition of Ar gas injection. The atomic process between the impurity ions and the plasmas can be calculated and simulated by Stand Alone Non-Corona (SANCO) transport code developed in Joint European Torus (JET).[9] From the line-integrated signals, tomography reconstruction performance was also evaluated with the Phillips-Tikhonov (P-T) regularization method. From the ratio of each combination of reconstruction images filtered by various Be foil thicknesses, 2-D T_e images were compared as well.

II. INSTALLATION OF 4-ARRAY SXR SYSTEM

The four-array system of SXR diagnostics has been designed and installed on KSTAR D-port. Two vertical and two

[a)]Contributed paper, published as part of the Proceedings of the 20th Topical Conference on High-Temperature Plasma Diagnostics, Atlanta, Georgia, USA, June 2014.

[b)]Present address: National Fusion Research Institute, Daejeon 305-806, Republic of Korea.
[c)]Author to whom correspondence should be addressed. Electronic mail: wchoe@kaist.ac.kr.

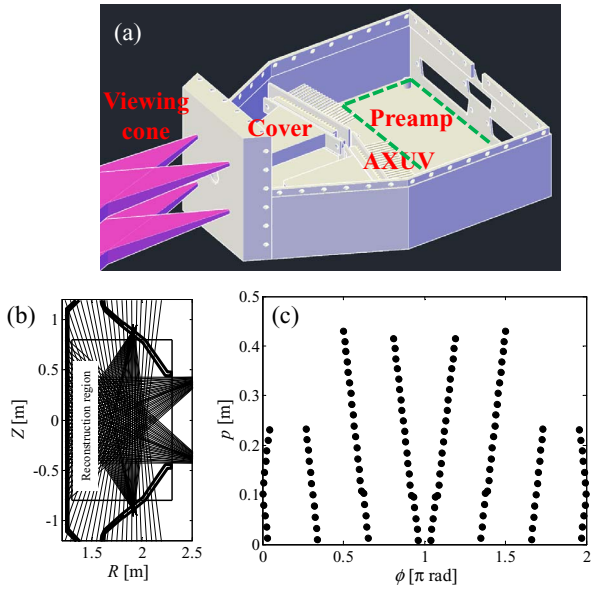

FIG. 1. (a) Schematic of a detector head of four-array SXR diagnostic system, (b) line of sight for each detector, and (c) result of coverage test.

horizontal arrays were mounted on the opposite side of the plasmas behind the passive plate and D-port cassette wall, respectively. Fiber-glass insulated wire was adopted in the vacuum circumstance. Each array contains 32 viewing chords and each chord has two different Be filter sets, so that the multi-energy method should be applied as illustrated in Fig. 1(a). The spatial resolution of 2 cm is guaranteed at the center of the plasmas as described in Fig. 1(b). V-shaped layout in detector head can contribute to the effective coverage in reconstruction area as plotted in p-ϕ diagram (Fig. 1(c)). The current-to-voltage convertor with gain of 10^6 V/A is arranged near the AXUV detector for high signal-to-noise ratio. The thicknesses of Be filter sets were chosen to be 50 μm and 250 μm optimized in T_e measurement, which will be explained in Sec. V.

III. CALIBRATION OF DETECTORS

The spectra of X-ray tube (MOXTEK MAGNUM® 50 kV TUB00050-1) were analyzed by a Si p-i-n diode detector (AMPTEK XR-100CR) with an energy resolution of 150 eV in the photon counting mode. A Fe-55 isotope was utilized in front of the diode to find the exact position of 5.9 keV.[10] The experimental conditions without photon overflow problem are listed in Table I. Considering the experimental configurations, the X-ray bremsstrahlung spectra emitted from the X-ray tube were reconstructed as depicted in Fig. 2(a), including the silver (Ag) K-edge line radiation of 22.1 keV and 24.94 keV. The response of AXUV-16ELG to the X-ray tube in conditions of bias voltages (10–40 kV) and

TABLE I. The experimental configuration without a photon pile-up problem for each bias voltage.

Voltage (kV)	Distance (mm)	Al filter (mm)	Slit area (mm^2)	Collecting time (s)
10	200	0	0.3	9.30
15	200	0	0.3	7.99
20	200	0.2	0.3	9.03
25	200	0.2	0.3	8.55
30	430	1	...	9.20
35	430	1	...	9.45
40	430	1	...	9.29

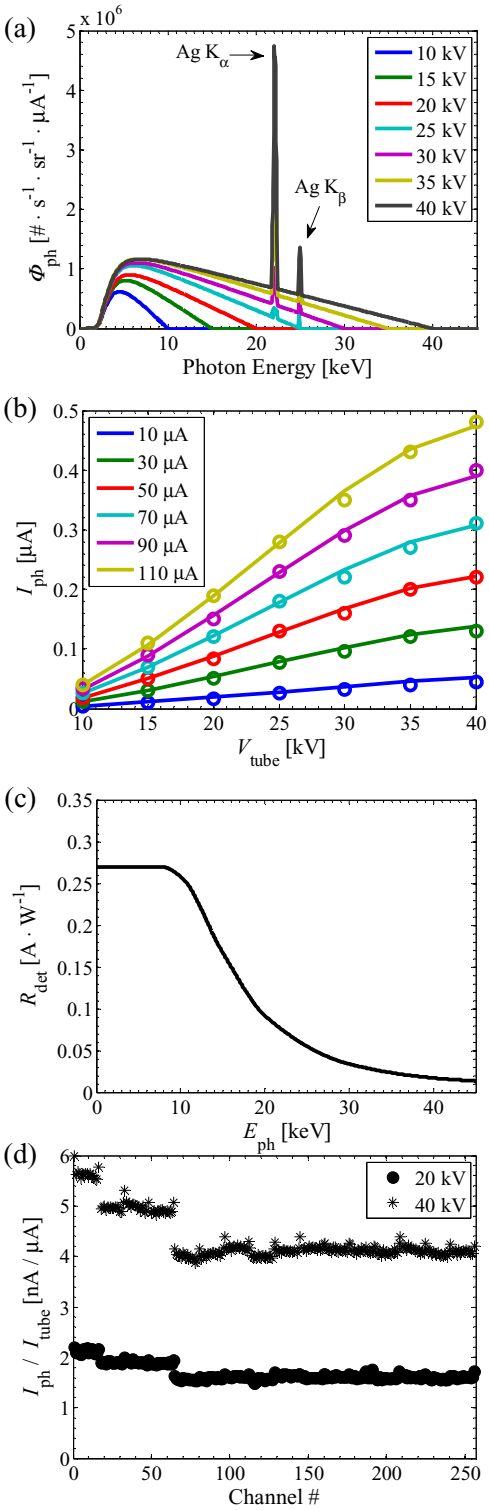

FIG. 2. (a) The photon flux emitted from the tube as a function of photon energy at various X-ray tube bias voltages. They are normalized in terms of the solid angle and beam current. Measured AXUV signals (solid lines) and simulation results (circles) as a function of (b) the bias voltage. (c) The responsivity curve of AXUV detector and (d) the relative calibration factors for each detector element.

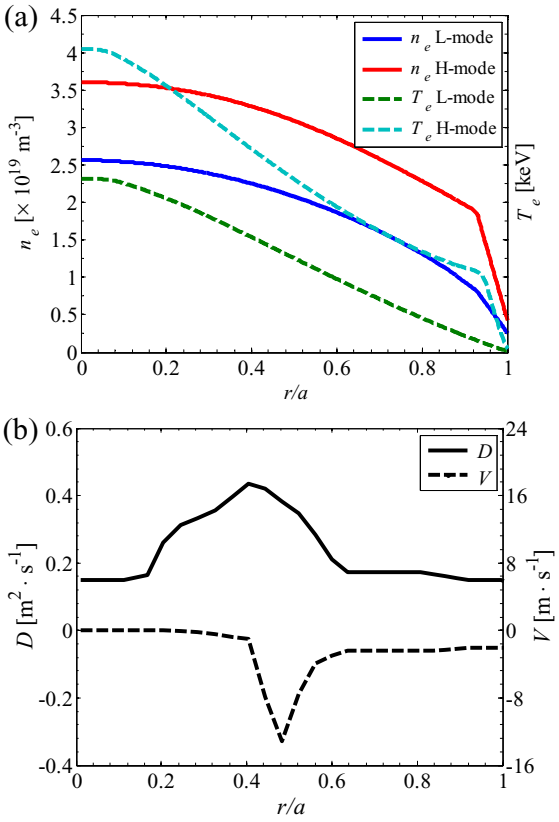

FIG. 3. (a) Typical KSTAR L-mode and H-mode n_e and T_e profiles. (b) Diffusion coefficient (D) and convection velocity (V) of Ar impurity are obtained from KSTAR L-mode discharge (#7566).[12]

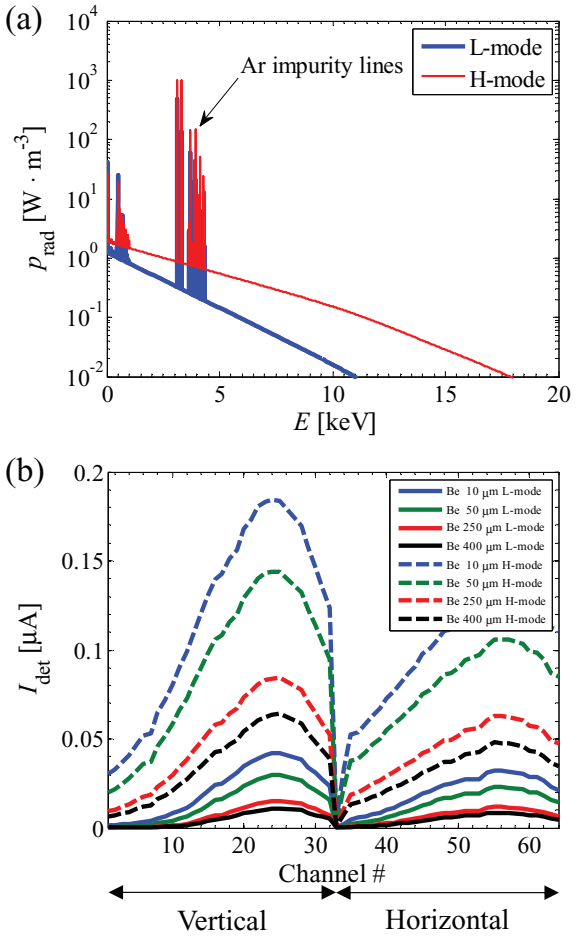

FIG. 4. (a) X-ray radiation spectra in core when Ar impurity density has a peak value. (b) Signal levels filtered by Be 10 μm (blue), 50 μm (green), 250 μm (red), and 400 μm (black) foils in KSTAR L-mode (solid line) and H-mode (dashed line).

beam current (10–110 μA) is plotted in Fig. 2(b). It is shown that the photodiode signal saturates beyond 35 kV, which means lower responsivity at a higher photon energy. Empirically, the AXUV detector responsivity was found as described in Fig. 2(c). For 256 channels of all detectors, the responsivity and the tube current (10–110 μA) have a linear relation, and the slopes are plotted in Fig. 2(d). There is some different responsivity among the arrays. The database of the responsivity for all detector elements will be used for relative calibration factors.

IV. SIGNAL ESTIMATION FOR KSTAR PLASMAS

A. Modelling of X-ray radiation in KSTAR

Typical KSTAR L-mode and H-mode n_e and T_e profiles are employed for modeling the X-ray radiation: bremsstrahlung, recombination, and line radiation as plotted in Fig. 3(a). Since the KSTAR plasma facing component is made of graphite, carbon (C) is the most important impurity. However, the line radiation of C is cut by Be filters below 1 keV, then it only affects Z_{eff}. Ar impurity is frequently used for X-ray imaging crystal spectroscopy in KSTAR[11] and as trace particles to study their transport,[12] therefore, the situation of Ar gas-puffing experiment is considered with total amount of 3×10^{17} Ar atoms, the puffing duration of 20 ms, and the recycling factor of 0.7. While impurity penetrating, the atomic process between Ar and plasmas was calculated by the SANCO transport code based on the typical n_e, T_e, diffusion coefficient (D), and convection (V) profiles in KSTAR L-mode as shown in Fig. 3(b). Since the collision frequency between Ar and main ions is much lower than that between Ar and electron, the ion temperature (T_i) profile is insensitive to the line radiation. Therefore, the equality of $T_i = T_e$ is assumed. The transport coefficients (D, V) in H-mode were imported from ASDEX-U.[13]

B. Signal estimation

As accumulating in the core plasma, Ar impurity concentration will reach peak density profile. The core ($r/a = 0$) X-ray radiation spectra in L-mode and H-mode are described in Fig. 4(a) at the peak time. The line-integrated signals filtered by Be 10 μm, 50 μm, 250 μm, and 400 μm are depicted in Fig. 4(b). The channel number from 1 to 32 lays on the vertical array, and the others are on the horizontal array. The signal levels are in the range from several tens to a few hundreds of nA. The current-to-voltage preamplifier gain of 10^6 V/A is sufficient producing a few hundreds of mV.

V. TOMOGRAPHY RECONSTRUCTION

Two-dimensional soft X-ray profiles filtered by the Be foil sets are reconstructed by the P-T tomography method.

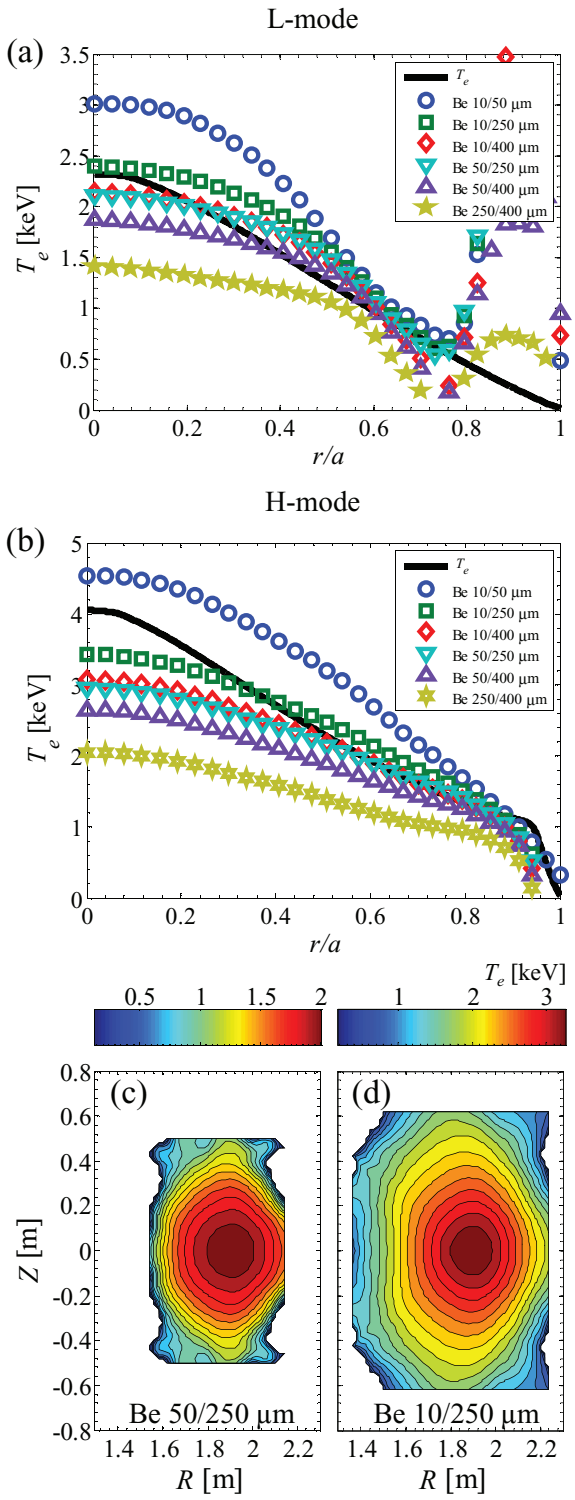

FIG. 5. Comparison between input T_e profile and calculation result by the multi-energy method in (a) L-mode and (b) H-mode. The best choice for the T_e measurement is (c) Be 50/250 μm and (d) Be 10/250 μm in L-mode and H-mode, respectively.

The P-T regularization method has better performance for accurate results and noise immunity than maximum entropy method, because the relation between adjacent pixels is concerned.[3] Assuming continuum radiation in the multi-energy method, the ratio between two images with different Be filters is related with electron temperature. There are six cases of the ratio sets that can visualize 2-D images of electron temperature. The radial profile of T_e calculation is compared in Figs. 5(a) and 5(b). The best choices of the T_e calculation map in 2-D are Be 50/250 μm and 10/250 μm pairs in L-mode and H-mode, as depicted in Figs. 5(c) and 5(d), respectively. The T_e measurement with 10/50 μm is somewhat overestimated, since it can be affected by Ar impurity line radiation in the low energy level. Due to the low signal levels by Be 250/400 μm, the result is underestimated by 40% and 50% in L-mode and H-mode.

VI. CONCLUSION

The four-array SXR diagnostic system was designed, fabricated, and installed in KSTAR with capability of the multi-energy method. For the X-ray detection, photo-diode (AXUV16-ELG) was chosen and calibrated with an X-ray tube. To estimate signals from KSTAR plasmas, a simple model with SANCO prediction was employed with Ar impurity. By the multi-energy method, 2-D T_e images can be derived from the ratio between combinations of reconstructed SXR images with various Be foils. Since the method ignores the impurity line radiation, the error of T_e calculation can arise with respect to the injected Ar impurities. It is identified that Be 50/250 μm and 10/250 μm sets are the best choices for 2-D T_e diagnostics in KSTAR L-mode and H-mode, respectively. Including detector calibration and tomography reconstruction tests, the optimization of proper filter sets for the SXR diagnostics is essential for Ar transport study. For the next step, the iron (Fe) impurity will be considered for the precise calculation.

ACKNOWLEDGMENTS

This research was supported by National R&D Program through the National Research Foundation of Korea (NRF) funded by the Ministry of Science, ICT, of Republic of Korea (NRF-2014M1A7A1A03045092).

[1]J. Kim and W. Choe, New Phys.: Sae Mulli **47**, 306 (2003).
[2]J. Kim, S. H. Lee and W. Choe, Rev. Sci. Instrum. **77**, 10F513 (2006).
[3]S. H. Lee, J. Kim, J. H. Lee, and W. Choe, Curr. Appl. Phys. **10**, 893 (2010).
[4]S. H. Lee, K. B. Chai, S. Jang, W.-H. Ko, J. Kim, D. Seo, J. Lee, I. N. Bogatu, J.-S. Kim, and W. Choe, Rev. Sci. Instrum. **83**, 10E512 (2012).
[5]L. Delgado-Aparicio, K. Tritz, T. Kramer, D. Stutman, M. Finkenthal, K. Hill, and M. Bitter, Rev. Sci. Instrum. **81**, 10E303 (2010).
[6]K. Tritz, D. J. Clayton, D. Stutman, and M. Finkenthal, Rev. Sci. Instrum. **83**, 10E109 (2012).
[7]E. M. Hollmann, L. Chousal, R. K. Fisher, R. Hernandez, G. L. Jackson, M. J. Lanctot, S. V. Pidcoe, J. Shankara, and D. A. Taussig, Rev. Sci. Instrum. **82**, 113507 (2011).
[8]OPTO DIODE CORP.; see http://optodiode.com.
[9]L. Lauro-Taroni *et al.*, in *Proceedings of the 21st EPS Conference on Controlled Fusion and Plasma Physics*, Montpellier, 1994, p. 102.
[10]D. Pacella, D. Mazon, A. Romano, P. Malard, and G. Pizzicaroli, Rev. Sci. Instrum. **79**, 10E322 (2008).
[11]S. G. Lee, J. G. Bak, U. W. Nam, M. K. Moon, Y. Shi, M. Bitter, and K. Hill, Rev. Sci. Instrum. **81**, 10E506 (2010).
[12]J. Hong *et al.*, A3 Foresight Program Workshop on Critical Physics issues Specific to Steady State Sustainment of High-Performance Plasmas, Beijing, 2013.
[13]S. de Peña Hempel, R. Dux, A. Kallenbach, H. Meister, and ASDEX Upgrade Team, in *Proceedings of the 24th EPS Conference on Controlled Fusion and Plasma Physics*, Berchtesgaden, 1997, p. 1401.